Development of a hybrid gamma camera based on Timepix3 for nuclear industry applications

Guillaume Amoyal, Vincent Schoepff, Frédérick Carrel, Maugan Michel, N. Blanc de Lanaute, J.C. Angélique

Development of a hybrid gamma camera based on Timepix3 for nuclear industry applications

G. Amoyal[(a)], V. Schoepff[(a)], F. Carrel[(a)], N. Blanc de Lanaute[(b)], M. Michel[(a)], J.C. Angélique[(c)]
[(a)] *Université Paris-Saclay, CEA, List, F-91120 Palaiseau, France*
[(b)] *MIRION TECHNOLOGIES (CANBERRA) SAS, 6 Avenue du Vieil Etang 78180 Montigny-Le-Bretonneux, France*
[(c)] *Normandie Univ., ENSICAEN, UNICAEN, CNRS/IN2P3, LPC Caen, 14000 Caen, France*

ABSTRACT

A prototype of hybrid gamma imager has been developed, based on a single Timpex3 readout chip hybridized with a 1 mm thick cadmium telluride semiconductor. This prototype combines coded-aperture imaging spectrometry and Compton imaging techniques to perform hybrid gamma imaging. It associates and takes advantage of both techniques to locate gamma emitters. The prototype is designed to be portable and compact in order to ease its field use. In this work, we present experimental results obtained with this prototype in coded-aperture imaging spectrometry mode, Compton imaging mode, and hybrid gamma imaging.

I. INTRODUCTION

Gamma imaging is a technique well adapted for the remote localization of radioactive sources. It presents a real interest in several application fields: decommissioning of nuclear facilities, nuclear waste management, and radiation protection in Nuclear Power Plants (NPP) or Homeland Security. This technique can simultaneously provide qualitative (spatial localization of radioactive sources) and quantitative information (radioactive hot spot intensities). Using gamma camera reduces the dose received by operators and consequently achieves the ALARA principle ("As Low As Reasonably Achievable"). There are two gamma imaging techniques for the localization of gamma emitters: coded-aperture imaging and Compton imaging [1][2]. Most of the gamma cameras are based on these approaches, requiring a pixelated detector.

Gamma camera with coded-aperture relies on a spatial modulation technique. The coded-aperture consists of a matrix made of transparent and non-transparent elements with a specific pattern, and is placed between the radioactive source and the detector. A source object projects the pattern of the coded-aperture on the detector; this projection is called a shadowgram. The reconstruction of the radioactive source is achieved by applying the knowledge of the coded-aperture pattern to the shadowgram [1]. A spectrometric criterion can be used to discriminate radioactive hotspots according to their energies, this criterion is used to carry out coded-aperture spectro-imaging. This imaging technique performs well in terms of sensitivity and spatial resolution, especially for photons with energy lower than 100 keV. However, its field-of-view is limited by the coded-aperture geometry, and its performances decrease as the energy of the incoming photons increase (due to sensing volume measuring efficiency).

Compton cameras rely on the Compton scattering kinematics. If an incident photon interacts two or more times in the detector, it is possible to locate a radioactive source. Indeed, the energy deposited during the first interaction allows calculating the first scatter angle, while the interaction position allows estimating the direction of the incident photons. The first scatter angle and the direction infer a cone, the radioactive source is on the surface of said cone. The intersection of several cones thus corresponds to the position of the radioactive source. The Compton imaging technique has the advantage of covering a theoretical field-of-view of 4π sr. However, because of the Compton kinematics, Compton camera performances are strongly degraded for incident energies lower than 100 keV. Moreover, the incident photon energy must be known a priori and on top of that, the quality of the localization is directly correlated to the spectrometric performances of the Compton gamma camera. In addition, it is also required to be able to identify coincidences within the sensitive area.

The purpose of this study is to develop a hybrid gamma camera prototype combining coded-aperture imaging with Compton imaging techniques. One of the interests of such an imager is to combine, in a single system, the benefits of both techniques and to mitigate at the same time associated limitations. A second interest concerns the multiplication of information sources for the localization of radioactive sources, because it opens interesting possibilities for the algorithmic reconstruction step.

The developments carried out in this study consisted in combining the two imaging techniques mentioned above around the Timepix3 chip, hybridized with a 1 mm cadmium telluride semiconductor.

This article gives an overview of the experimental results obtained with Timepix3 with coded-aperture spectro-imaging, Compton imaging, and with hybrid gamma imaging. First, the main characteristics of Timepix3 are described, then descriptions of coded-aperture spectro-imaging and Compton imaging are detailed, and the specifications of the radioactive sources used for this study are described. Following, the experimental results obtained with both imaging techniques are presented. An example emphasizing the interest of hybrid gamma imaging is also given. Finally, future developments related with this topic are underlined at the end of the article.

II. Material and Methods

A. Timepix3

In 2013, CERN developed Timepix3 [3], that works as an event-based readout chip. The Timepix3 hybrid-pixel readout chip is a matrix made of 256 × 256 square-shaped pixels with 55 µm pitch. Timepix3 can be hybridized to several types of semiconductor, such as Si or CdTe with thicknesses up to 5 mm. In each pixel, it simultaneously records the Time-over-Threshold (ToT) that gives access to deposited energy [4], and the time-of-arrival (ToA) with a time resolution of 1.5 ns. Therefore, the Timepix3 chip has the necessary requirements to perform coded-aperture spectro-imaging and Compton imaging, which are: energy measurement, fast time sampling, and fine pixelisation pitch to precisely locate interaction position.
For this study, we used a Timepix3 hybridized with a 1 mm thick N-on-P cadmium telluride semi-conductor equipped with Schottky contacts, operating in electron collection mode under -300 V bias. The power supply of the chip, the semiconductor bias, and the communication with the acquisition computer are carried out by the Katherine readout system developed in cooperation between Faculty of Electrical Engineering, University of West Bohemia and IEAP, CTU [5]. In order to simplify the terminology in our paper, the term "Timepix3" will refer to the Timepix3 readout chip hybridized to the cadmium telluride semiconductor.
The energy calibration was set following the method described in [6], and was performed in the energy range from 15 keV to 1.3 MeV. The energy calibration allows for spectrometric performances such that for photons with an energy > 80 keV, energy resolution is < 10 %, and the relative error on measured energy is < 0.5 % for photons with an energy > 25 keV [7].

B. Coded-aperture spectro-imaging

For several years, CEA List has been designing coded aperture systems, such as GAMPIX [8]–[11], that has been industrialized by MIRION Technologies under the commercial name of iPIX [12], [13]; and lately Nanopix, the smallest gamma imager based on coded-aperture in the world. Both of those technologies rely on a pixellated detector, associated with a MURA coded-aperture [14]. For our prototype, we selected a 4 mm-thick tungsten alloy, rank 7, MURA coded-aperture. This choice is based on our expertise in the GAMPIX system, this coded-aperture is the best compromise between angular resolution and measurement sensitivity (here defined as the minimum time to locate a radioactive source) [15]. The distance between the coded mask and the detector is 1.6 cm, which corresponds to a squared field-of-view of 50°×50°. Figure 1 is a photography of Timepix3 equipped with its MURA coded-aperture.
The so-called "mask/anti-mask" procedure (MAM procedure) is used, and consists in carrying out a second measurement after rotating the mask by 90°. The MAM procedure enables a suppression of the gamma background generated by radioactive sources located out of the field-of-view of the gamma camera [14].
The decoded image is obtained using the algorithm described in [14]. This method consists in an autocorrelation between the decoding function described by the coded-aperture pattern, and the measured shadowgram. In our case, the sensitive area is the Timepix3 detector, and is made of 256×256 pixels; therefore, the decoded image has the same size and is made of 256×256 pixels. During the decoding process, the spectrometric information is also taken into account in order to deploy coded-aperture spectro-imaging. This feature enables to obtain a decoded image corresponding to a specific energy region of interest, which is defined by the end-user. To do so, during the decoding process, a criterion on the energy deposited by each event is applied.

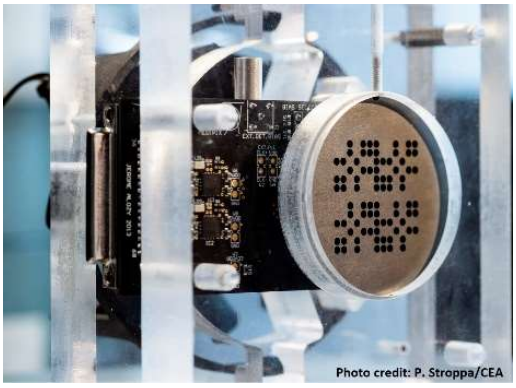

Figure 1: Timepix3 and its MURA coded-aperture. Photo credit: P. Stroppa/CEA.

C. Single detector Compton imaging

The most popular configuration for Compton imaging is based on a two detectors structure: a first detector, "the scatterer", in which the Compton scattering process will occur, associated to a second detector, the "absorber", in which the scattered photon will be absorbed [2]. Compton imaging takes advantage of scattering kinematics, as illustrated in Figure 2 (a). The energy deposited during the scattering process determines the scattering angle (see Figure 2 (a)), then the interaction position determine the direction

of the incident gamma-ray. The position of the radioactive source is set on the surface of a cone, which apex corresponds to the scattering event position, as illustrated in Figure 2 (b).
Considering several interactions from a unique source, multiple Compton cones are determined and their overlap coincide is the source location, as shown in Figure 3 (a). Results shown in Figure 3 and Figure 4 are obtained with Monte-Carlo simulations of a Cs-137 radioactive source, with a two detectors structure (300 µm-thick Si material, associated with a 1 mm-thick CdTe material, 1 cm apart from each other). The Cs-137 radioactive source is set at 1 m in the upper-right part of the system's field-of-view. Those results are obtained considering a "perfect" system, in which there is no uncertainty, either on positions or on energies measurements.
In this work, the Compton cones are projected on a pixelated half-sphere, which corresponds to a 2π sr field-of-view. The algorithm used to calculate the projection of Compton cones consists in a simple back projection (SBP) algorithm, as described in [2]. Once the Compton cones are projected on the pixelated half-sphere, the position of the radioactive source is highlighted by applying a threshold at 50% of the maximal number of counts in the image, associated with a two-dimensional Gaussian filtering at 1 sigma, as illustrated in Figure 3 (b). The Gaussian filtering is done so as to apply mathematical regularization.

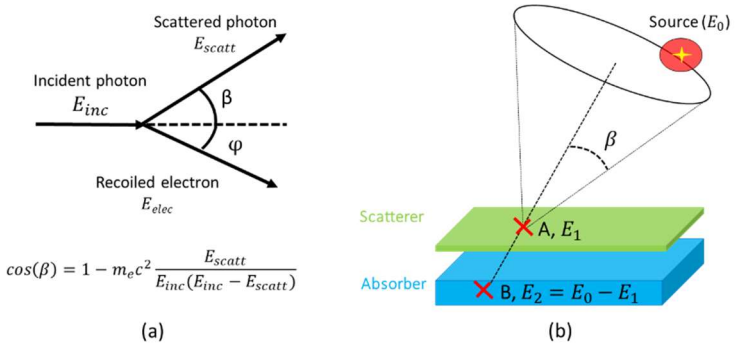

Figure 2: (a) Compton scattering diagram and equation; (b) determination of a Compton cone through interactions locations in scatterer and absorber detectors.

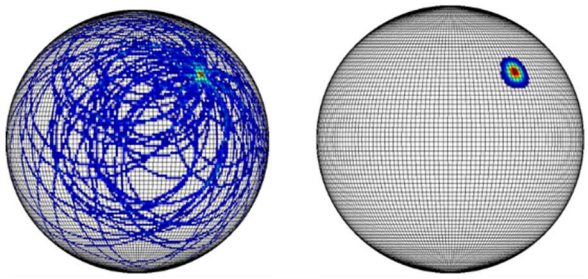

Figure 3: Representations of the location of a radioactive source using the simple back projection algorithm, (a) without filtering, (b) with a 50% threshold and 1 sigma Gaussian filtering.

We also have implemented the possibility of modifying the pixel grid of the half-sphere on which the Compton cones are projected. This allows for a trade-off between the angular resolution and the sensitivity, as illustrated in Figure 4. This kind of trade-off makes sense in the case of on-field measurements, for which the measurement times may be limited, making it impossible to obtain sufficient statistics for fine pixelisation. Projections shown in Figure 4 result from Monte-Carlo simulations with the same configuration as the one shown in Figure 3 (a). The Cs-137 radioactive source is located 1 m from the system, in the middle of the system's field-of-view.

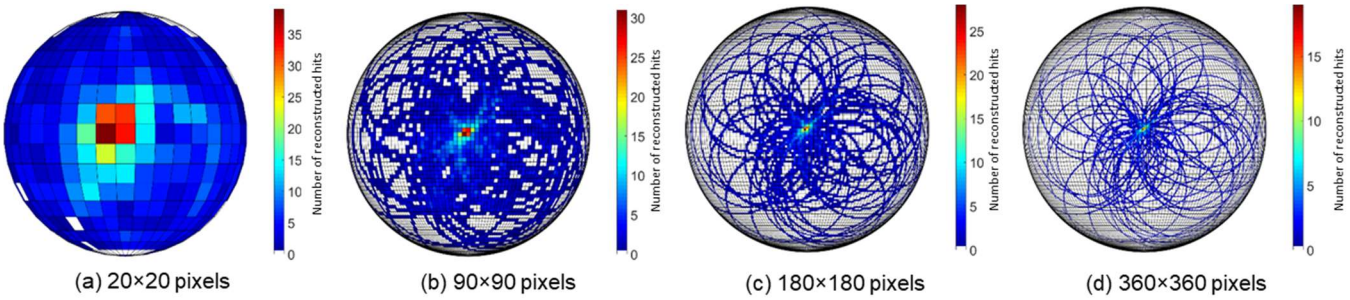

Figure 4: Impact of the half-sphere pixel grid on which are projected the Compton cones: (a) 20×20 pixels; (b) 90×90 pixels; (c) 180×180 pixels; (d) 360×360 pixels.

In this study, we used a "single detector configuration", in which, said detector is thick enough for Compton scattering and absorption to occur in the same detection volume. We decided to develop such a configuration because it offers benefits in terms of compactness and price. Moreover, using a single detector configuration also avoids the need to synchronize two detectors. The single detector configuration is illustrated in Figure 5FIGURE 5.

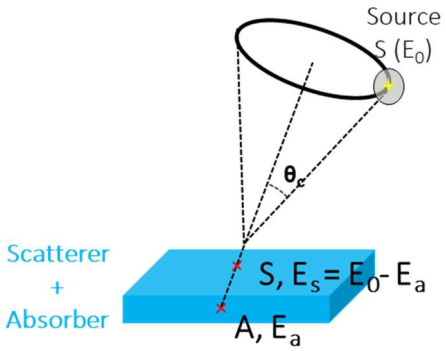

Figure 5: Illustration of the single detector configuration for Compton imaging.

In such a configuration, there is no direct information on the nature of the identified Compton events, *i.e.* which interaction corresponds to Compton scattering and which corresponds to absorption. In the case of the single detector configuration, the temporal resolution of Timepix3 (1.5 ns) is higher than the photon time-of-flight between two interactions. Therefore, there is no direct *a priori* on the interactions. The sequence of interactions shall be reconstructed from the information on the positions and energies of both interactions. In the case where one of the two energies has an energy greater than the energy of the Compton edge, this interaction will necessarily correspond to the absorption. For all other cases, it is not possible to know directly which interaction corresponds to which event.

A deterministic algorithm, based on the Klein-Nishina formula was developed in [16]. This algorithm consists in probabilistically determining which event is associated to each of the two interactions (Compton scattering or absorption). The function describing the probability density of a photon to be scattered at a certain an angle, is calculated taking the solid angle fraction into account, and is given by Equation (II-1) [16]. In Equation (II-1), β is the Compton scattering angle; and $K(\beta, E)$ (called the Klein-Nishina coefficient [17]) is the probability that a photon with an energy E scatters at an angle β.

$$P(\beta) \propto \int_0^{2\pi} K(\beta, E) \sin\beta \, d\varphi \;\propto 2\pi \cdot K(\beta, E) \sin\beta \qquad \textit{(II-1)}$$

The construction of the Compton cones, enabling for the localization of radioactive sources, requires both energy measurements and information on the interaction positions. In the case of a single detector configuration, there is no direct information on the depth of interaction. In order to minimize the uncertainty on the Compton cone axes, a practical solution consists in considering only the pairs of events separated by at least a certain distance. A study has been carried out by Monte-Carlo simulation with MCNP6 2.0 [18] to determine this optimal distance. This study consisted in simulating a CdTe volume, with dimensions similar to those of Timepix3 described in paragraph II.A. The CdTe volume is irradiated by a source emitting photons with an energy of 662 keV (Cs-137), located at 1 m in front of the detection volume. For those Monte-Carlo simulations, energy resolutions of Timepix3 [7]; and its 55 µm pixelisation are taken into account.

Figure 6 shows the evolution of the number of Compton cones, as a function of the distance between the position of Compton scattering and absorption. As expected, an increase in the distance between the two interactions implies a decrease in the number of Compton cones.

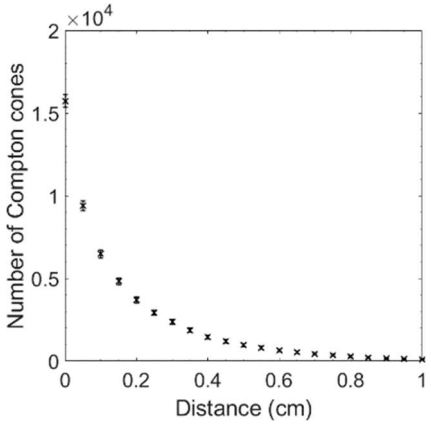

Figure 6: Evolution of the number of Compton cones as a function of the minimal distance between Compton scattering position and absorption position. Error bars are given at three sigmas.

However, an increase in the distance between the two interactions lowers the angular resolution associated with the reconstructed source. Figure 7 shows three reconstructed images using the SBP algorithm for different distances between the Compton scattering position and the absorption position. Figure 8 is a plot of azimuthal FWHM at the reconstructed position of the source, as a function of the distance between the Compton scattering position and the absorption position. In order to compare the FWHM values, the same number of Compton cones (100) is used for the reconstruction for each position. This value was chosen because it corresponds to the number of Compton cones obtained for the maximum distance between the interaction positions. For a distance of 1 cm between two interactions, 100 Compton cones are obtained for a Cs-137 having emitted 1.2×10^{13} photons (equivalent to an exposure time of 33 hours using a 100 MBq source). A greater number of Compton cones would imply an even greater time of exposure, which would be incompatible with end-user constraints. An increase in the minimum distance between interactions implies a decrease in FWHM at the reconstructed source position. Since FWHM at the reconstructed source position corresponds to the angular resolution in degree, it equates to a lower angular resolution.
Therefore, a compromise must be found between the minimum distance between interactions positions and the sensitivity of the Compton gamma camera. The value corresponding to the best compromise between the number of Compton cones and the angular resolution was found to be 5 mm.

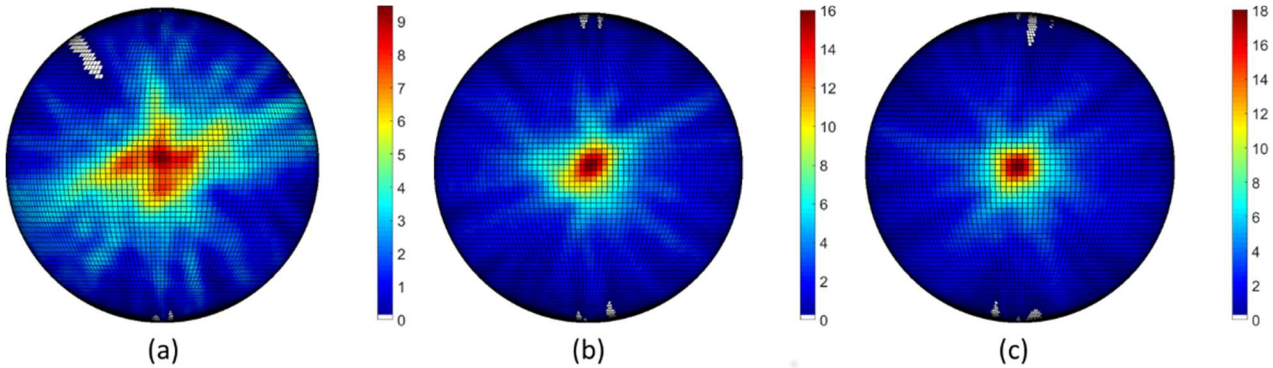

Figure 7: Reconstructed image with the SBP algorithm of a Cs-137 source positioned in front of a single detector configuration, for different distances between the Compton scattering position and the absorption position ((a) 1 mm, (b) 5 mm, (c) 9.5 mm). The images are reconstructed using 100 Compton cones, without any filtering. The colour scale corresponds to the number of Compton cones intersection.

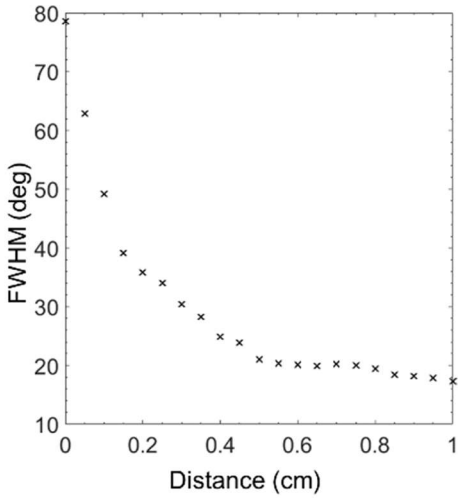

Figure 8: Plot of the azimuthal FWHM (i.e the angular resolution in degree) of the reconstructed hotspot against the distance between the positions of Compton scattering and absorption. For each distance, 100 Compton cones are used to reconstruct the position of the source.

D. Radionuclide

In order to assess the possibility of achieving coded-aperture spectro-imaging and Compton imaging using Timepix3, several measurements have been carried out using different radionuclides chosen for they are the most commonly encountered in the nuclear industry. Activities and experimental equivalent dose rates at 1 m are summarized in table 1. The different energies used to identify/locate those radionuclides are also specified.

Table 1: List of activities and measured equivalent dose rates of the different radionuclides used to evaluate the localization performances of the Timepix 3 gamma camera prototype. The characteristic energy lines used for gamma imaging associated with each radionuclide are listed.

Radionuclide	Activity [MBq]	Experimental equivalent dose rate at 1 m [$\mu Sv.h^{-1}$]	Characteristic energies used for gamma imaging [keV]
Am-241	73.8	0.95	59.5
Ba-133	23.3	1.64	303; 356
Na-22	1.5	0.57	511; 1022
Cs-137	34.5	2.92	662
Co-60	20.0	6.11	1173; 1332

III. Experimental measurements

A. Coded-aperture spectro-imaging using Timepix3

Several studies have been carried out to evaluate the coded-aperture imaging performances of the GAMPIX gamma camera [8], [9], [11], [15]. The GAMPIX gamma camera is a prototype of coded-aperture imaging system. It is industrialized by MIRION Technologies under the name of iPIX [19]. The detector of the GAMPIX camera is a Timepix detector hybridized to a 1 mm thick CdTe semiconductor. The dimensions of the semiconductor, as well as the pixelisation of the detector, are identical between the GAMPIX gamma camera detector and the here discussed prototype gamma camera based on Timepix3. In addition, the operating modes of the two detectors are almost identical. Therefore, the experimental evaluation of the localization capabilities with Timepix3 proposed in this study will not be exhaustive. For in-depth studies on this matter, see [8], [13]– [19].

In order to evaluate Timepix3 ability for coded-aperture spectro-imaging, the following measurement has been carried out: two radioactive sources (Am-241 and Ba-133) have been simultaneously positioned at 1 m within the field- of-view of our prototype. The Am-241 source is positioned in the upper-part of the field-of-view, whereas the Ba-133 source is positioned in the lower-part. The measurement is carried out following the MAM procedure (see paragraph II.B): 30 min in mask mode, and 30 min in anti-mask mode.

Figure 9 shows the decoded images without any energy discrimination (a), and when Ba-133 characteristic energies are selected (b), and when the Am-241 characteristic energy is selected (c). Without energy selection, only the Ba-133 radioactive source is reconstructed. With energy selection applied, both sources can be separately identified.

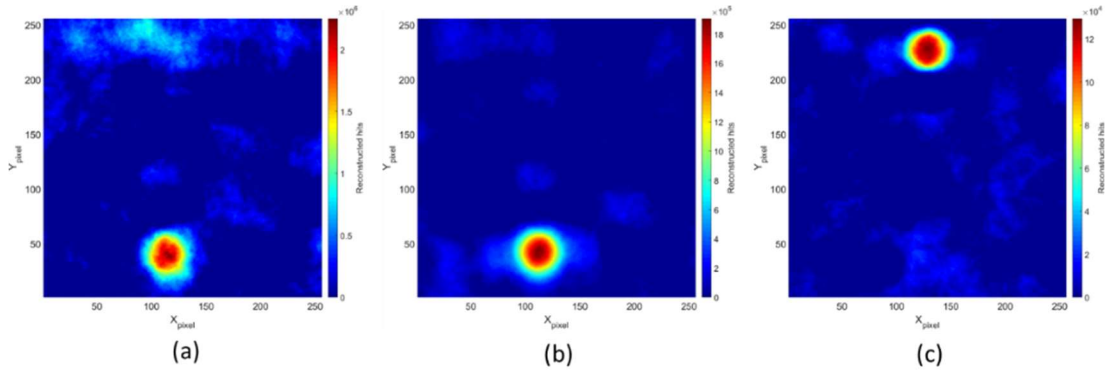

Figure 9: Coded-aperture imaging decoded images) when: (a) no energy criterion is used (a); (b) Ba-133 characteristic lines are selected (81 keV, 303 keV, 356 keV); (c) Am-241 characteristic line is selected (59.5 keV). The measurement is carried out with MAM procedure. Sources are positioned at 1 m from the Timepix3 detector, with an exposure time of 1 h (30 min in mask mode, and 30 min in anti-mask mode).

A limit of coded-aperture imaging concerns the reconstruction of artefacts when a radioactive source is located at the periphery of the fully coded field-of-view of the coded-aperture [20]. Figure 10 (a) illustrates the field-of-view and the coding fraction of a coded-aperture gamma camera. Figure 10 (b) shows the reconstruction of a Cs-137 source positioned in said position. In this case, there is an uncertainty about the true position of the Cs-137 source (hot spot split into two diametrically opposite parts). A knotty case may be encountered while performing *in-situ* measurements, if the radioactive source is located in the partially coded field-of-view, then it will be not located in the decoded image.
In the case of an unknown environment, it is not possible to know what the «true» position. The solution to counter this effect is to perform an additional Compton measurement that allows the identification of the "real" radioactive source position.

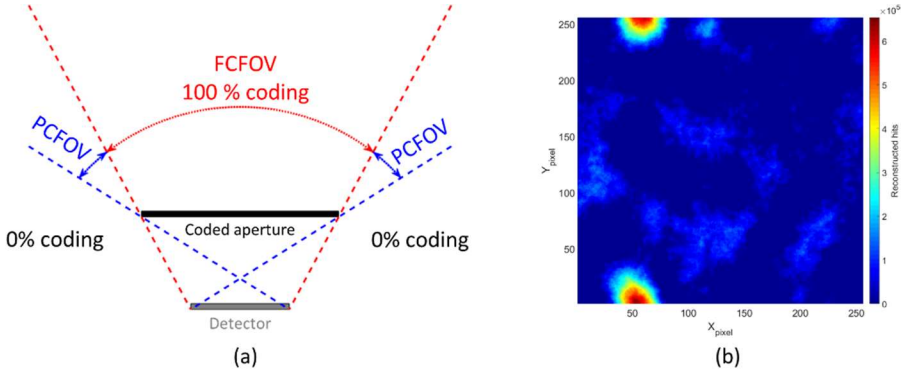

Figure 10: (a) Field-of-view and coding fraction illustration of a coded-aperture gamma camera showing the Fully Coded Field-Of-View (FCFOV), and the Partially Coded Field-Of-View (PCFOV). (b) Localization of a Cs-137 source, using coded-aperture imaging, positioned at the border of the fully coded field-of-view. The source is positioned in the upper part of the coded-aperture field-of-view. The distance between the source and the detector is 1 m. The measurement is carried out with the MAM procedure with a total exposure time of 1 h (30 min in mask mode, and 30 min in anti-mask mode).

B. Compton imaging with Timepix3

Experimental validation of the Timepix 3's ability to locate radioactive hot spots in Compton mode have been carried out with the following radionuclides: Am-241, Ba-133, Na-22, Cs-137, and Co-60. Characteristics in terms of activity and equivalent dose rate are summarized in table 1.

1) Single source localization and sensitivity evaluation

In this paragraph, we present experimental results obtained for a single radionuclide source positioned in the 2π Timepix 3 field-of-view. First, we evaluated the ability to locate a single radionuclide and the associated sensitivity. The source/detector distance is 1 m and exposure time 1 h. This protocol was applied for each radionuclide. Experimental results demonstrate that Timepix3 is able to locate Ba-133, Na-22, Cs-137, and Co-60 for the investigated positions as illustrated in Figure 11. However, it was not possible to locate Am-241: this is mainly due to the energy resolution of the detector (5.65 keV at 59.5 keV) combined with the Doppler broadening effect [21]. The combination of these two parameters increases the uncertainty on the calculation of the Compton scattering angle.

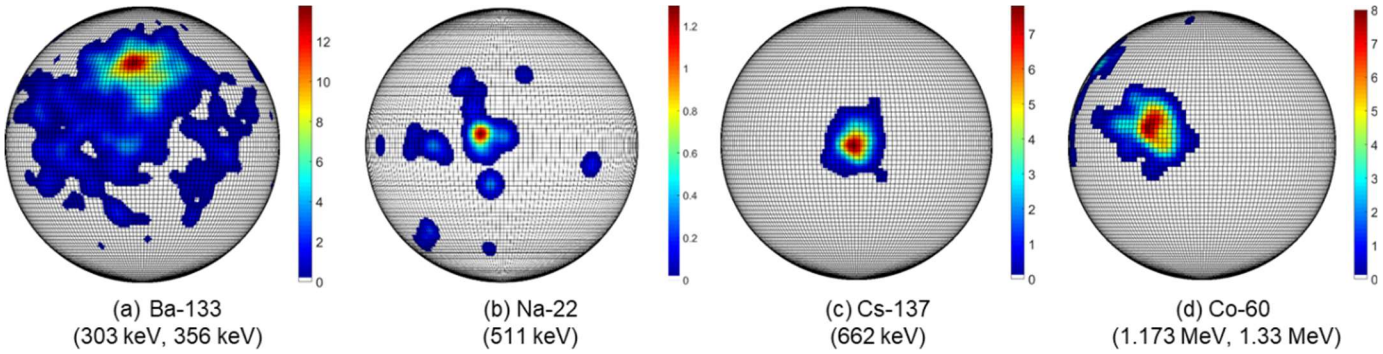

Figure 11: Compton imaging results obtained with the Timepix3 detector for different radionuclides positioned in a 2π sr field-of-view: (a) Ba-133, (b) Na-22, (c) Cs-137, (d) Co-60. The energy lines used to reconstruct the images are given for each radionuclide. For each measurement, the distance between the Timepix3 detector and the radioactive source is 1 m, total exposure time is 1 h.

After validating the experimental feasibility of Compton imaging with Timepix 3, we focused on the sensitivity in this specific acquisition mode. For this evaluation, the radioactive source is positioned at the center of the field-of-view. Sensitivity is qualitatively evaluated according to a visual criterion on the reconstructed image. The sensitivity indicator is defined as the minimum exposure time necessary to correctly locate a single radioactive source.

Sensitivity evaluation is obtained by observing the reconstructed images for acquisition time bins of 60 seconds. Sensitivity depends on the pixel grid of the reconstructed image. Therefore, we evaluated sensitivity for three different pixelisations of the reconstructed image: 20×20, 90×90 and 180×180 pixels. Figure 12 shows the reconstructed images with the 20×20, 90×90, and 180×180 pixelisations of the half-sphere, for which the best sensitivity value was assessed reached. For these experiments, we used a Cs-137 source positioned at the center of the Compton field-of-view.

Sensitivity values for Ba-133, Cs-137, and Co-60 sources, and for all three pixelisations of the half-sphere of, are presented in table 2. Timepix3 here experimentally demonstrates is capability to locate the Ba-133, Cs-137, and Co-60 sources at 1 m, considering acquisition time between 240 and 1560 seconds depending on the pixelisation of the reconstructed space and the nature of the source. These results confirms that it is possible to achieve shorter measurement times by reducing the number of pixels (*e.g.* with a 20×20 pixelisation).

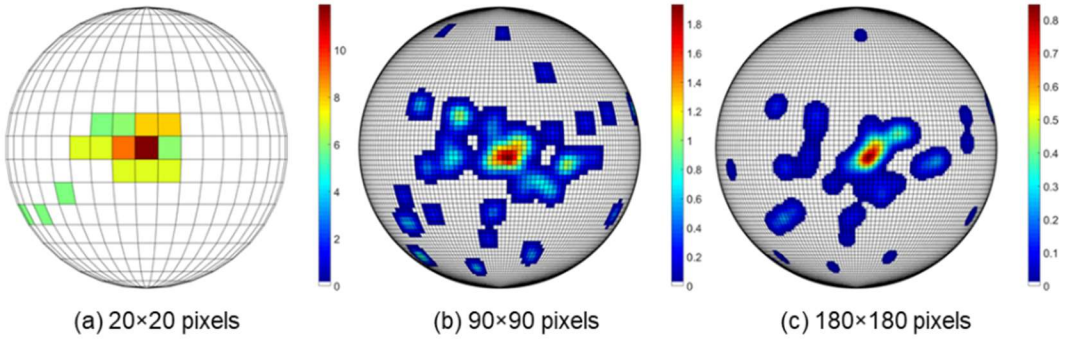

Figure 12: Example of reconstructed images corresponding to the qualitatively evaluated sensitivity limit. Pictures are obtained with a Cs-137 source positioned at the center of the field-of-view, at a distance of 1 m. Values are given as pixelisation and exposure time: (a) 20×20 pixels, 180 s; (b) 90×90 pixel, 300 s; (c) 180×180 pixels, 360 s.

Table 2: Sensitivity evaluation for different radionuclides at a distance of 1 m, for pixel grids of the reconstructed space of 20×20, 90×90 and 180×180 pixels.

Radionuclide	Equivalent dose rate at 1 m [μSv.h^{-1}]	Sensitivity evaluation [s]		
		20×20 pixels	90×90 pixels	180×180 pixels
Ba-133	1.6	300 +/- 60	360 +/- 60	660 +/- 60
Cs-137	2.9	240 +/- 60	300 +/- 60	360 +/- 60
Co-60	6.1	840 +/- 60	1080 +/- 60	1560 +/- 60

2) Multiple source measurements

As with coded-aperture spectro-imaging, it is possible to perform energy-selective reconstructions by considering the full energy peaks present in the energy spectrum. In the nuclear industry, it is usual for the measured spectrum to be made of several radionuclides. For this reason, it is important to evaluate how Timepix3 is capable of separating radionuclides according to their energies. In order to evaluate this feature, two measurements have been carried out.

The first measurement consisted in simultaneously positioning a Ba-133 source and a Cs-137 source, 1 m from the detector, within the Timepix 3 field-of-view, with an acquisition time of 2 h. The Ba-133 source is positioned on the left side of the field-of-view,

while the Cs-137 source on the top side. Figure 13 (a) shows the measured energy spectrum corresponding to this experimental configuration: the peaks used for radionuclides identification/location are highlighted. Figure 13 shows the reconstructed images when the energies of Ba-133 (b) and Cs-137(c) are selected.

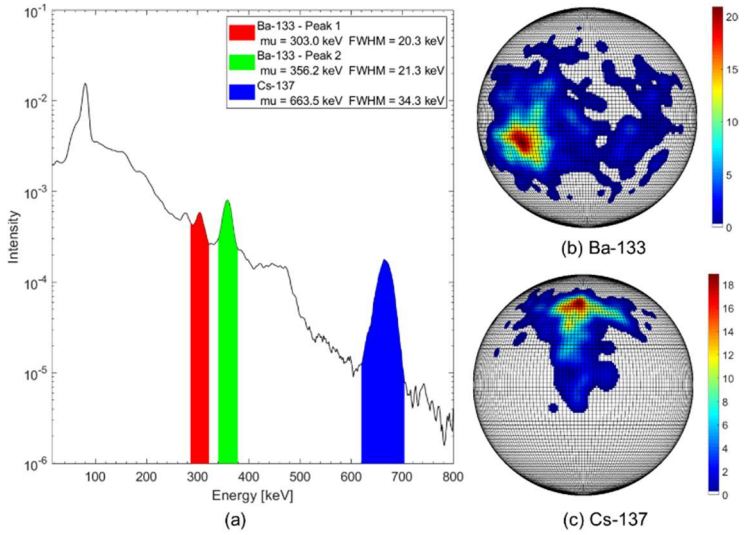

Figure 13: Multiple source localization with Timepix3 working in Compton mode (Ba-133 and Cs-137 simultaneously positioned within the field-of-view): (a) the measured energy spectrum, the peaks used for a considered radionuclide are highlighted. For a given energy peak "mu" corresponds to the mean energy; (b) reconstructed image when energy lines of Ba-133 are selected; (c) reconstructed image when energy line of Cs-137 is selected.

A second measurement was carried out by placing a Cs-137 source and Co-60 source simultaneously within the Timepix3 field-of-view. The distance from the radioactive sources to the detector is 1 m, and the acquisition time is 2 h. The Cs-137 source is positioned on the left side of the detector's field-of-view. The Co-60 source is positioned in the right part of the field-of-view. Figure 14 (a) shows the energy spectrum and the peaks of interest with a specific colour code. Figure 14 shows the reconstructed images when the energies of Cs-137 (b) and Co-60 (c) are selected.

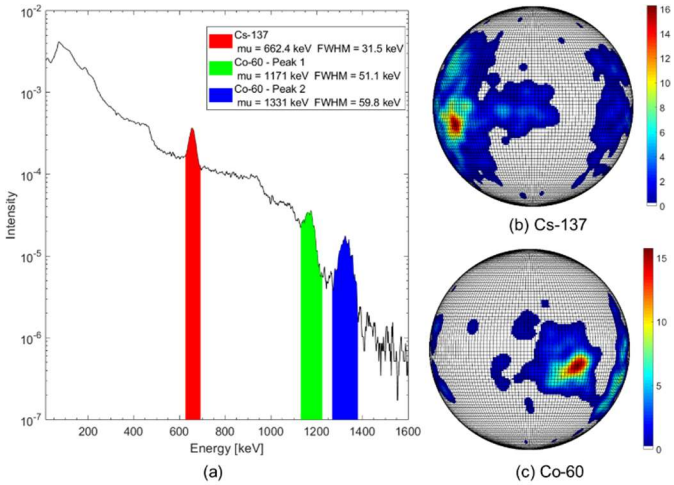

Figure 14: Multiple sources localization with Timepix3 and Compton mode (Cs-137 and Co-60 simultaneously positioned within the field-of-view): (a) measured energy spectrum, with peaks used for radionuclide identification are coloured; (b) reconstructed image when energy line of Cs-137 is selected; (c) reconstructed image when energy lines of Co-60 are selected.

C. Hybrid gamma imaging with Timepix3

In order to evaluate hybrid imaging with Timepix3, an experimental measurement was performed by simultaneously positioning an Am-241 source within the field-of-view of the coded-aperture prototype, and a Cs-137 source within its partially coded field-of-view. This measurement aims to illustrate the interest of a hybrid gamma imager, and to illustrate how to take advantage of each gamma imaging technique.

The measurement setup of this experiment is described hereinafter.The distance between the sources and the detector is 1 m. For practical reasons, measurements are performed separately: first in ”Compton imaging” mode and then in ”coded-aperture imaging“ mode. Acquisition time for the Compton imaging measurement is 1 hour. The acquisition time for coded-aperture imaging measurement is 30 minutes in mask position, and 30 minutes in anti-mask position. The exposure time for coded-aperture could be reduced to one minute, but in order to have enough counting statistics it was decided to carry out a one-hour measurement.
Figure 15 (a) and (b) show the decoded images obtained by selecting, respectively, the energy lines associated to Am-241 (59.5 keV) and Cs-137 (662 keV) using coded-aperture spectro-imaging. The decoded images are projected on the pixelated half sphere also used for Compton imaging. The Am-241 source is measured at the correct position; however, there is an uncertainty related to the position of the Cs-137 source (two hotspots are recontructed). The actual position of the Cs-137 source is in the lower-left side of the field-of-view, as shown by the Compton image in Figure 15 (c).
In this measurement, coded-aperture imaging is used for the localization of an Am-241 source, and Compton imaging is used for the localization of a Cs-137 source. First, the Am-241 can not be localized with our system and Compton imaging (see paragraph III.B.1), highlighting one interest of the coded-aperture imaging information. Regarding the Cs-137 source, it is positionned within the partially coded field-of-view of the coded aperture, therefore an uncertainty on its position remains with coded-aperture imaging (see paragraph III.A and Figure 15 (b)), highlighting one interest of the Compton imaging information.
This measurement is an example of the contribution of coded-aperture imaging for the localization of the Am-241 source, and of Compton imaging for the localization of the Cs-137 source.

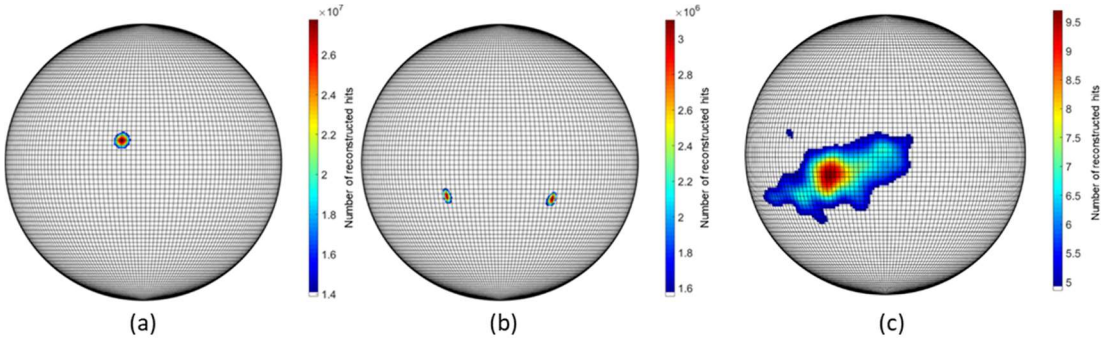

Figure 15: (a) and (b), Localization using coded-aperture spectro-imaging of an Am-241 source positioned in the fully coded field-of-view and a Cs-137 source positioned at the border of the fully coded field-of-view of the coded-aperture. Energy windows are set at the characteristic energy gamma emissions of the radionuclides (59.5 keV for Am-241 and 662 keV for Cs-137). A 50% threshold is applied on the decoded images. (c) Compton imaging location of the Cs-137 source with Timepix3. A Gaussian filtering and 50% threshold are applied.

Once the positions of the radioactive sources have been identified, the decoded images associated with each of the two imaging modes can be superposed on a visible image. The main interest of this aspect is the visualization of the imaging results. The visible image is a photograph taken with a fisheye camera, or wide-angle camera (*i.e.* 2π sr field-of-view), well adapted to Compton acquisition modes. Figure 16 shows the superposition of the visible image, the coded-aperture image, associated with the Am-241 (Figure 15 (a)), and the Compton image, associated with the Cs-137 source (Figure 15 (c)). In order to improve visibility, a grid pattern has been added, corresponding to a reconstructed space pixelisation of 20×20 pixels.

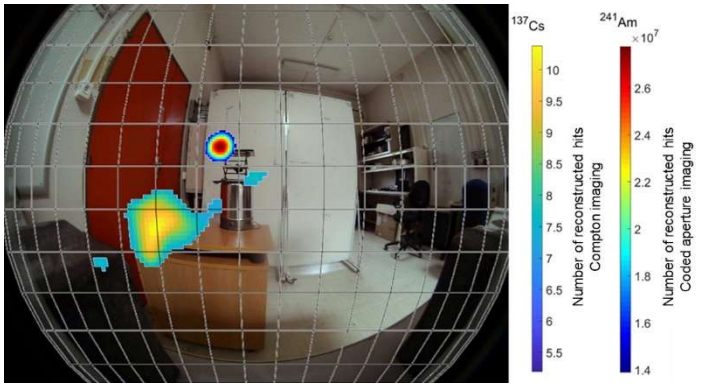

Figure 16: Example of the use of the hybrid gamma imaging with Timepix3. Superposing the wide-angle visible image, the decoded image in the coded-aperture mode with a 50% threshold and an energy window corresponding to Am-241, and the decoded image in the Compton mode with a 70% threshold and an energy window corresponding to Cs-137 (yellow).

IV. Conclusion and future developments

The objective of this work was to develop a prototype hybrid gamma imager, combining coded-aperture and Compton imaging techniques, dedicated to applications in the nuclear industry. The different localization measurements in coded-aperture imaging and Compton imaging with the developed prototype demonstrated the feasibility to build a hybrid gamma imager based on Timepix3. An experimental validation of the prototype is detailed. In this test, an Am-241 source was positioned in the fully-coded field-of-view of the coded-aperture, and a Cs-137 source was placed in the partially-coded field-of-view of the coded-aperture. The experimental results demonstrate the prototype performances and thus emphasis the benefits of a hybrid gamma imager.

The various developments carried out in this work open up several prospects for the further development of a hybrid imager based on Timepix3 technology. First, the sensitivity and angular resolution capabilities of the prototype in Compton imaging mode need to be evaluated. Indeed, only its localization capabilities have hereby been demonstrated.

Another perspective concern hybrid imaging. At this stage, information from Compton and coded-aperture imaging is only normalized and added-up A study must be conducted to make the best use of both sources of information. On the other hand, it has been shown by Lynde [22], that the combination of a neutron-sensitive conversion layer with a tungsten coded-mask around the Timepix detector allows neutron imaging. The developments led by Lynde, thus paved the way for a double-particle hybrid imaging system, sensitive to both X and gamma rays and neutrons.

References

[1] M. J. Cieślak, K. A. A. Gamage, and R. Glover, "Coded-aperture imaging systems: Past, present and future development – A review," *Radiat. Meas.*, vol. 92, pp. 59–71, 2016, doi: 10.1016/j.radmeas.2016.08.002.

[2] M. Frandes, B. Timar, and D. Lungeanu, "Image Reconstruction Techniques for Compton Scattering Based Imaging: An Overview," *Curr. Med. Imaging Rev.*, vol. 12, pp. 95–105, 2016.

[3] T. Poikela *et al.*, "Timepix3: a 65K channel hybrid pixel readout chip with simultaneous ToA/ToT and sparse readout," *J. Instrum.*, vol. 9, no. 05, pp. C05013–C05013, 2014, doi: 10.1088/1748-0221/9/05/c05013.

[4] J. Jakubek, "Energy-sensitive X-ray radiography and charge sharing effect in pixelated detector," *Nucl. Instruments Methods Phys. Res. Sect. A Accel. Spectrometers, Detect. Assoc. Equip.*, vol. 607, no. 1, pp. 192–195, 2009, doi: 10.1016/j.nima.2009.03.148.

[5] P. Burian, P. Broulím, M. Jára, V. Georgiev, and B. Bergmann, "Katherine: Ethernet Embedded Readout Interface for Timepix3," *J. Instrum.*, vol. 12, no. 11, pp. C11001–C11001, 2017, doi: 10.1088/1748-0221/12/11/c11001.

[6] J. Jakubek, "Precise energy calibration of pixel detector working in time-over-threshold mode," *Nucl. Instruments Methods Phys. Res. Sect. A Accel. Spectrometers, Detect. Assoc. Equip.*, vol. 633, no. SUPPL. 1, pp. S262–S266, 2011, doi: 10.1016/j.nima.2010.06.183.

[7] G. Amoyal, Y. Menesguen, V. Schoepff, F. Carrel, N. Blanc de Lanaute, and J. C. Angélique, "Evaluation of Timepix3 Si and CdTe hybrid pixel detectors spectrometric performances on X- and gamma rays," *under Rev. Process*.

[8] F. Carrel *et al.*, "GAMPIX: a new generation of gamma camera for hot spot localisation," *2010 ISOE Int. Symp.*, no. November, pp. 17–19, 2010.

[9] M. Gmar, M. Agelou, F. Carrel, and V. Schoepff, "GAMPIX: A new generation of gamma camera," *Nucl. Instruments Methods Phys. Res. Sect. A Accel. Spectrometers, Detect. Assoc. Equip.*, vol. 652, no. 1, pp. 638–640, 2011, doi: 10.1016/j.nima.2010.09.003.

[10] H. Lemaire *et al.*, "Implementation of an imaging spectrometer for localization and identification of radioactive sources," *Nucl. Instruments Methods Phys. Res. Sect. A Accel. Spectrometers, Detect. Assoc. Equip.*, vol. 763, pp. 97–103, 2014, doi: 10.1016/j.nima.2014.05.118.

[11] G. Amoyal, V. Schoepff, F. Carrel, V. Lourenco, D. Lacour, and T. Branger, "Metrological characterization of the GAMPIX gamma camera," *Nucl. Instruments Methods Phys. Res. Sect. A Accel. Spectrometers, Detect. Assoc. Equip.*, vol. 944, p. 162568, 2019, doi: 10.1016/j.nima.2019.162568.

[12] K. Amgarou, A. Patoz, D. Rothan, and N. Menaa, "iPIX: A New Generation Gamma Imager for Rapid and Accurate Localization of Radioactive Hotspots," no. October, pp. 3–5, 2014.

[13] K. Amgarou *et al.*, "A comprehensive experimental characterization of the iPIX gamma imager," *J. Instrum.*, vol. 11, no. 8, 2016, doi: 10.1088/1748-0221/11/08/P08012.

[14] S. R. Gottesman and E. E. Fenimore, "New family of binary arrays for coded aperture imaging," *Appl. Opt.*, vol. 28, no. 20, p. 4344, 1989, doi: 10.1364/ao.28.004344.

[15] F. Carrel *et al.*, "GAMPIX: A new gamma imaging system for radiological safety and homeland security purposes," *IEEE Nucl. Sci. Symp. Conf. Rec.*, pp. 4739–4744, 2012, doi: 10.1109/NSSMIC.2011.6154706.

[16] D. Xu, Z. He, C. E. Lehner, and F. Zhang, "4-pi Compton imaging with single 3D position-sensitive CdZnTe detector," in *Proceedings of SPIE - The International Society for Optical Engineering - Hard X-Ray and Gamma-Ray Detector Physics VI*, 2004, vol. 5540, pp. 144–155, doi: 10.1117/12.563905.

[17] O. Klein and Y. Nishina, "Über die Streuung von Strahlung durch freie Elektronen nach der neuen relativistischen Quantendynamik von Dirac," *Zeitschrift für Phys.*, vol. 52, no. 11, pp. 853–868, 1929, doi: 10.1007/BF01366453.

401 [18] J. T. Goorley *et al.*, “Initial MCNP6 Release Overview - MCNP6 version 1.0,” 2013.
402 [19] K. Amgarou, A. Patoz, D. Rothan, and N. Menaa, “iPIX: A New Generation Gamma Imager for Rapid and Accurate
403 Localization of Radioactive Hotspots,” *Conf. IAEA Symp. Int. Safeguards Link. Strateg. Implement. People Vienna*, vol.
404 IAEA–CN–22, Oct. 2014.
405 [20] P. M. Charalambous, A. J. Dean, J. B. Stephen, and N. G. S. Young, “Aberrations in gamma-ray coded aperture imaging,”
406 *Appl. Opt.*, vol. 23, no. 22, p. 4118, 2009, doi: 10.1364/ao.23.004118.
407 [21] A. Zoglauer and G. Kanbach, “Doppler broadening as a lower limit to the angular resolution of next-generation Compton
408 telescopes,” *X-Ray Gamma-Ray Telesc. Instruments Astron.*, vol. 4851, no. March, p. 1302, 2003, doi: 10.1117/12.461177.
409 [22] C. Lynde *et al.*, “Demonstration of coded-aperture fast-neutron imaging based on Timepix detector,” *Nucl. Instruments*
410 *Methods Phys. Res. Sect. A Accel. Spectrometers, Detect. Assoc. Equip.*, vol. 954, no. July 2018, p. 161373, 2020, doi:
411 10.1016/j.nima.2018.10.051.